

Optimization of Crystal Violet Adsorption by Chemically Modified Potato Starch Using Response Surface Methodology

Bahrami, M. *, Amiri, M. J. and Bagheri, F.

Department of Water Engineering, Faculty of Agriculture, Fasa University,
P.O.Box 74616-86131, Fasa, Iran

Received: 04.09.2019

Accepted: 23.11.2019

ABSTRACT: In this research, a response surface methodology (RSM) was used to investigate the effects of independent parameters (pH, contact time, temperature, adsorbent dosage, and initial concentration of pollutant), their simultaneous interactions, and quadratic effects on crystal violet adsorption onto two starch based materials in the form of batch experiments. The characterizing results indicated that there is no significant difference between the potato starch and synthesized starch phosphate, as phosphorylation has not changed the crystalline structure of starch inside the granules. The maximum removal efficiency of crystal violet ions was obtained 99 % at the optimum adsorption conditions of initial concentration 213.54 mg/L, adsorbent dosage 0.25 g, contact time 14.99 min, temperature 15 °C, and initial pH of solution 9. RSM outputs showed that the maximum adsorption of crystal violet ions by could be achieved by raising pH and adsorbent dosage, and decreasing the initial crystal violet concentration. While temperature and contact time are not effective parameters in crystal violet removal from aqueous solutions using synthesized starch phosphate. Generally, the RSM model is suitable to optimize the experiments for dye elimination by adsorption, where the modified starch phosphate would be an effective adsorbent for treating crystal violet solution.

Keywords: Adsorption; Dye removal; Optimization; Water treatment.

INTRODUCTION

The utilization of dyes is very significant in many industries, such as textile, paper, printing, leather, food, cosmetics, and pharmacy, etc., which produce noticeable amounts of color wastewater. Nowadays, the release of colored effluents into water resources creates many health and environmental problems. Dyes can affect aquatic plants and aquatic life and may cause violent loss to human beings including dysfunction of the central nervous system, liver, brain, kidneys, etc. Decolorization of dyes is too difficult

because of their complex structure and extant the aromatic rings, which make them carcinogenic and mutagenic. So, the elimination of color from effluents is a great concern for the researchers and environmentalists (Crini, 2006).

Crystal violet belongs to the class of triphenylmethane dyes that has been extensively used as a histological stain in veterinary medicine, bacteriostatic agent, and skin disinfectant. But, it is detrimental when inhaled or ingested and can make permanent blindness, kidney and respiratory damage, and skin irritation. Crystal violet as a cationic dye is more toxic than anionic

* Corresponding Author, Email: bahrami@fasau.ac.ir

dyes and it can simply react with cell membrane surfaces, concentrate in the cytoplasm, and enter into cells.

In recent decades, many methods have been represented for the removal of dyes from effluents such as ion exchange, reverse osmosis, electrochemical treatment, and adsorption (Kaur et al., 2015). Although the above-mentioned processes have been widely used, most of them have some disadvantages like high cost, using plenty of chemicals, waste long time, defective dye removal, production of non-biodegradable by-products and toxic sludge (Duraipandian et al., 2017). However, the adsorption method is one of the powerful treatment processes for the elimination of dyes as it is an inexpensive, highly effective, and simple method (Rabipour et al., 2016). The selection of the best type of adsorbent in terms of availability, high capacity rate, and applicability for multiple reuses is the main challenge in this wastewater treatment method.

Previous researches used conventional materials such as polyaniline nanoparticles (Saad et al., 2017), commercial activated carbons (Duraipandian et al., 2017), and organic resins for the elimination of crystal violet with success. However, their widespread use is restricted due to high costs. For this reason, alternative non-conventional materials including natural materials (clays, siliceous materials, and zeolites), waste materials from agriculture and industry (by-products), and biosorbents (peat, biomasses, polysaccharides) have been proposed and studied for their ability to remove dyes (Gil et al., 2011; Mundada and Brighu, 2016; Dehghani et al., 2017; Bharathi and Ramesh, 2013; Zehra et al., 2016; Sofu, 2019; Feira et al., 2018).

Biopolymer materials demonstrate more interest for a substitute as adsorbents due to their non-toxic nature, low cost, and biodegradability. Among the natural polymers, starch has been regarded as the most used polymer because of its physical and chemical properties such as special

polymeric construction, inherent biodegradability, superb sorption attributes towards a large range of contaminants, simplicity in availability, renewable source, and comparatively low cost (Olad et al., 2014; Gimbert et al., 2008). Linear amylose (poly- α -1,4-D-glucopyranoside) and branched amylopectin (poly- α -1,4-D-glucopyranoside and α -1,6-D-glucopyranoside) are forming constituent of semi-crystalline polysaccharide starch. Amorphous regions and crystalline shape of starch are because of amylose and amylopectin in its structure respectively. Due to the feeble adsorbing organization groups in the potato starch construction, it has limited dye adsorption capacity (Olad et al., 2014). However, starch by itself cannot be directly applied in adsorbing the dye because it has inherently no chelating or complexing abilities. Therefore, it is very necessary to modify the starch chemically to obtain effective adsorbents for dye removal from aqueous solution.

Herbal and natural materials have been used for the treatment of drinking water in rural areas in many developing countries (Bhattacharjee et al., 2013; Mumbi et al., 2018). Among the plant and natural materials in laboratory studies that have been proven the ability to coagulant, can mention the starch that is efficient in water turbidity removal (Shahriari and NabiBidhendi, 2012).

One of the crucial ideas of this study was to determine the optimum adsorption conditions using the response surface methodology (RSM) based on the central composite design (CCD). RSM is based on a combination of mathematical and statistical techniques that has been employed to change one independent variable (i.e., pH, temperature, time, initial concentration of the dye, and adsorbent dosages) while maintaining the others at a fixed level. Therefore, optimum conditions for desired responses can be predicted (Babaei et al., 2015; Amiri et al., 2018; Amiri et al. 2019; Shojaei et al., 2019). The

usual method for determination of optimum conditions for different parameters is expensive and time-consuming due to a large number of experiments. RSM (under Minitab 16 software) helps optimize the process parameters with a limited number of experiments.

This work aimed to optimize the removal of crystal violet from aqueous solution using synthesized starch phosphate as a novel adsorbent and to study the effect of pH, initial concentration of dye, contact time, temperature, and adsorbent dosage on the elimination of dye.

MATERIALS AND METHODS

In this study, two adsorbents including

potato starch powder (S) and synthesized starch phosphate (S-S) were used. Potato starch powder was purchased from Merck Chemical Co., Darmstadt, Germany. The S-S was synthesized by the procedure proposed by Sung et al. (2005). In brief, 100 g of potato starch and 30 g of disodium hydrogen orthophosphate anhydrous were dissolved into 100 mL of distilled water. Then, the mixture was continuously stirred for 20 min to disperse the grains of the materials, and finally, the contents were filtered and left at room temperature for 12 hours. Several physicochemical properties of the studied adsorbents are represented in Table 1.

Table 1. Physicochemical properties of studied adsorbents

Parameter	Starch powder	Synthesized starch phosphate
pH	6-7.5	7.25
Solubility	50 g/L	Insoluble in aqueous
Bulk density	300 Kg/m ³	534 Kg/m ³
Particle size	-	152 µm

Devices such as Perkin Elmer FT-IR (model Spectrum RXI) and Bruker D8 Advance with Cu-Ka over the 2θ range of 5°–85° were used for FTIR spectra as KBr pellets and XRD studies respectively. Both of SEM (Scanning Electron Microscope) and EDX (Energy-dispersive X-ray spectroscopy) analyses were carried out using a Tescan microscope, model Vega3. Before the experiment, the samples were coated by gold and carbon with Quorum model Q150R ES for SEM and EDX analyses, respectively.

Crystal violet used for this study was provided from Merck Chemical Co., Darmstadt, Germany (CI-42555, molecular formula C₂₅H₃₀ClN₃, molecular weight 407.99 g/mol, λ_{max} 590 nm) and used without further purification. The chemical structure of crystal violet is presented in Fig. 1. In this procedure, all the solutions were prepared by diluting the stock solution (1000 mg/L) with the proper volume of distilled water and the stock

solution was prepared by dissolving a specified weight of dye in 1000 mL of distilled water.

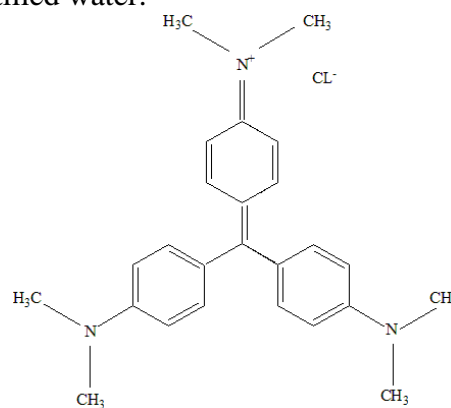


Fig. 1. Structure of crystal violet

The correlation among a group of controlled experimental factors and measured response based on one or more criteria is evaluated by RSM. Various important parameters were optimized by using the central composite design (CCD) of RSM. The experimental design was analyzed using the Minitab 16 software. Fitting the experimental data can be

described using a second-order polynomial response surface model:

$$y = \beta_0 + \sum_{i=1}^5 \beta_i x_i + \sum_{i=1}^5 \sum_{j>i}^5 \beta_{ij} x_i x_j + \sum_{i=1}^5 \beta_{ii} x_i^2 + \varepsilon \quad (1)$$

where 'y' is the predicted response (removal efficiency %), terms of β_0 , β_i , β_{ii} , β_{ij} , and ε illustrate the offset term, the linear effect,

the squared effect, the interaction effect, and the residual term respectively. x_i and x_j represent the coded independent variables (pH, temperature, time, initial concentration of pollutant, and the dose of adsorbents). The ranges and levels of the applied factors for the CCD are demonstrated in Table 2. Details of CCD and experimental conditions are represented in Tables S1 and S2 for different adsorbents (in supplementary material).

Table 2. The ranges of different parameters selected for the CCD of each adsorbent

Parameter	Adsorbent	Coded and real value				
		- α	-1	0	+1	+ α
pH	S	2	4	5.5	7	9
	S-S	2	4	5.5	7	9
T (°C)	S	20	30	40	50	60
	S-S	20	30	40	50	60
t (min)	S	15	45	67.5	90	120
	S-S	5	8	10	12	15
C ₀ (mg/L)	S	5	25	40	55	80
	S-S	30	100	150	200	250
C _s (g)	S	0.10	0.20	0.30	0.40	0.50
	S-S	0.03	0.10	0.15	0.20	0.25

Based on the RSM outputs (Tables S1 and S2), adsorption batch experiments were performed and the effect of the adsorption parameters including dose of adsorbents (C_s), initial concentration of pollutant (C₀), pH, temperature (T), and contact time (t) was studied on the crystal violet removal from aqueous solution. The crystal violet solutions were made according to the concentrations determined by RSM for each adsorbent from stock solutions. The effect of initial pH was assessed over the range 2-9 by adding 0.1 M HCl/ NaOH and was measured using a pH meter (HATCH, sension3). 10 mL of crystal violet solutions with different concentrations by various pHs were added into a 50 mL conical flask that washed with distilled water. Then a known amount of adsorbents in each experiment run was added into the solutions and stirred at 120 rpm unto a given time and temperature using incubator shaker from Fara Azma Co. Iran. In the end, the solutions were filtered by using Whatman

filter paper No. 41. The crystal violet dye concentrations before and after adsorption processes were analyzed by using a UNICO-2100 UV-Vis spectrophotometer (Perkin-Elmer 3030 instrument) at $\lambda_{\max} = 590$ nm. The standard calibration curve was achieved from the spectra of the standard solutions. The adsorption capacity and adsorption efficiency were calculated using the following formula respectively:

$$q_e = \frac{C_0 - C_e}{m} \times V \quad (2)$$

$$E = \frac{C_0 - C_e}{C_0} \times 100 \quad (3)$$

where C₀ and C_e (mg/L) are the initial liquid-phase and equilibrium concentrations of crystal violet, respectively. V (L) is the volume of the solution, m (g) is mass of the dry adsorbents, q_e (mg/g) and R (%) are the crystal violet uptake at equilibrium and removal efficiency of crystal violet, respectively.

RESULTS AND DISCUSSION

The FT-IR spectra of potato starch powder (S) and synthesized starch phosphate (S-S) before and after dye removal are represented in Fig. 2. The potato starch showed different perceptible absorbencies at 952, 1026, 1090 and 1164/cm, which were ascribed to C–O bond stretching. A characteristic peak occurred at 1638/cm, which presumably originates from tightly bound water present in the starch (Song et al., 2006). The band at 2930/cm is ascribed to the C-H stretching

vibration. The broad peak at about 3400/cm was attributed to the hydroxyl groups (O-H) of starch. According to Coates (2000), a characteristic broad feature in the range between 1250–1350/cm is attributed to stretching vibrations of organic phosphates (P=O stretch). According to Murúa-Pagola et al. (2009), no difference was observed between spectra of potato starch powder and S-S probably due to a strong dependence on hydration in stretching vibration of PO_2^{-2} group.

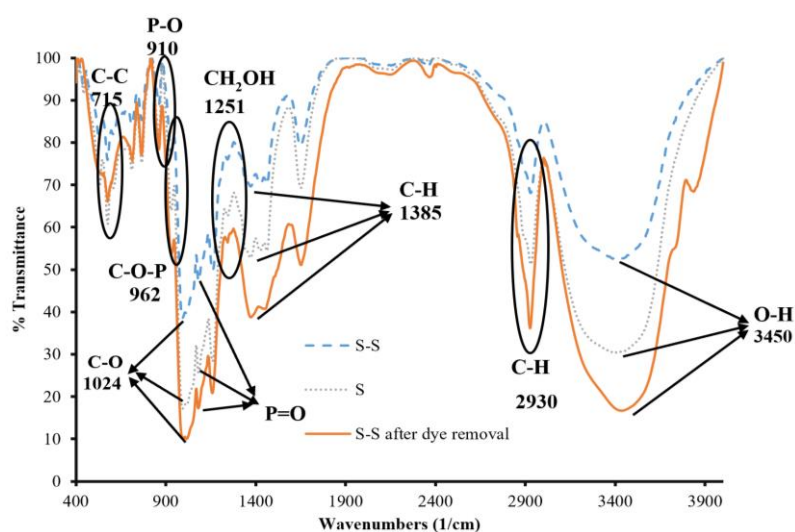


Fig. 2. FT-IR spectra of potato starch powder (S), synthesized starch phosphate (S-S) before and after dye removal

Comparing the FT-IR spectrum of S-S and S-S after adsorption of dye, it can be observed that some of the peaks are disappeared (503/cm) and some new peaks were bolded around 3742, 3848, and 2384/cm. Therefore, according to the spectrum in the adsorption process on the surface of S-S, the involvement of those functional groups is possible.

Scanning electron photomicrographs of potato starch powder and synthesized starch phosphate before and after crystal violet dye adsorption with three different magnifications of 10, 50, and 200 μm are exhibited in Fig. 3. As shown, there is no difference between the shape and size of starch granules before and after modification and also after dye removal.

However, SEM inquiries illustrated that the potato starch powder has a dispersed texture, whereas the synthesized starch phosphate has a concentrated structure (Figs. 3a and d).

According to the X-ray diffraction patterns of potato starch (S) and synthesized starch phosphate (S-S) represented in Fig. 4, they have a less crystalline structure. Results indicate the presence of three characteristic peaks for potato starch ($2\theta = 15.08^\circ, 17.05^\circ, \text{ and } 23.00^\circ$) and four characteristic peaks for synthesized starch ($2\theta = 15.181^\circ, 17.24^\circ, 18.53^\circ, \text{ and } 23.07^\circ$). As can be seen, there is no significant difference between the XRD patterns of potato and synthesized starches. This may be due to the presence of a semi-crystalline

structure of amylopectin inside the granules. It can be achieved that phosphorylation has not changed the crystalline structure of starch inside the granules.

As the above aforementioned, the experimental data was obtained by applying a special experimental run produced by the CCD while the assessed removal efficiency of crystal violet ions by

$$R = 18.82 + 32.73 \text{ pH} - 1.37 T - 0.21 t - 0.14 C_0 - 34.74 C_s - 2.32 \text{ pH}^2 + 0.023 T^2 + 0.0025t^2 - 0.127(\text{pH} \times t) - 0.0098(\text{pH} \times C_0) - 0.007(T \times t) - 2.81(\text{pH} \times C_s) - 0.001(T \times C_0) + 0.21(T \times C_s) - 0.002(t \times C_0) - 0.17(t \times C_s) + 0.495(C_0 \times C_s) \quad (4)$$

$$R = 93.918 + 4.267 \text{ pH} - 0.19 T - 0.694 t - 0.096 C_0 + 84.057 C_s - 0.339 \text{ pH}^2 + 0.002 T^2 - 310.434 C_s^2 - 0.005(\text{pH} \times T) + 0.041(\text{pH} \times t) + 0.006(\text{pH} \times C_0) + 0.005(T \times t) - 6.739(\text{pH} \times C_s) - 0.001(T \times C_0) + 0.698(T \times C_s) + 0.002(t \times C_0) - 2.287(t \times C_s) + 0.495(C_0 \times C_s) \quad (5)$$

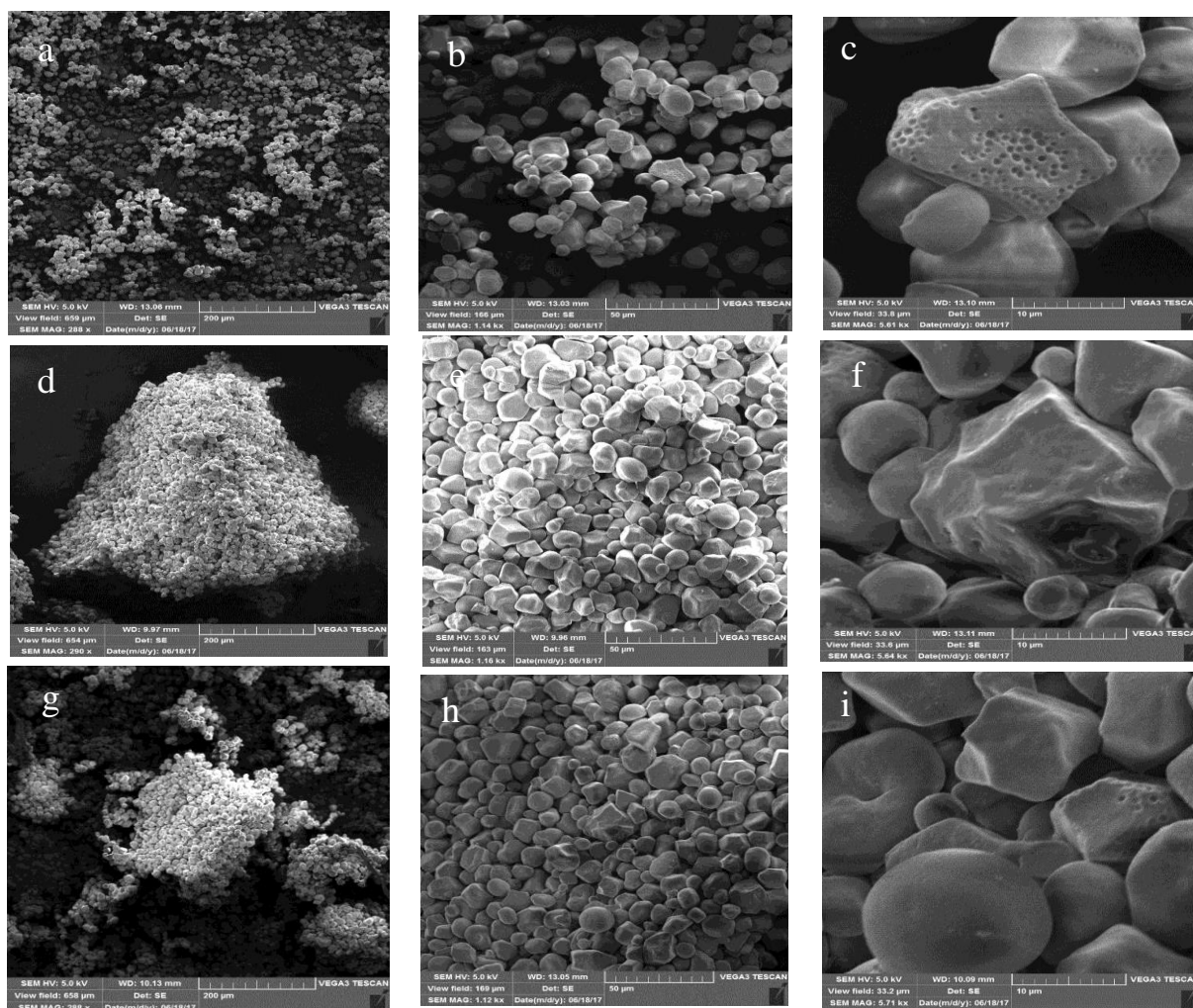


Fig. 3. Scanning electron micrographs of potato starch powder in (a) 200 μm , (b) 50 μm , and (c) 10 μm ; synthesized starch phosphate in (d) 200 μm , (e) 50 μm , and (f) 10 μm ; synthesized starch phosphate after dye adsorption in (g) 200 μm , (h) 50 μm , and (i) 10 μm

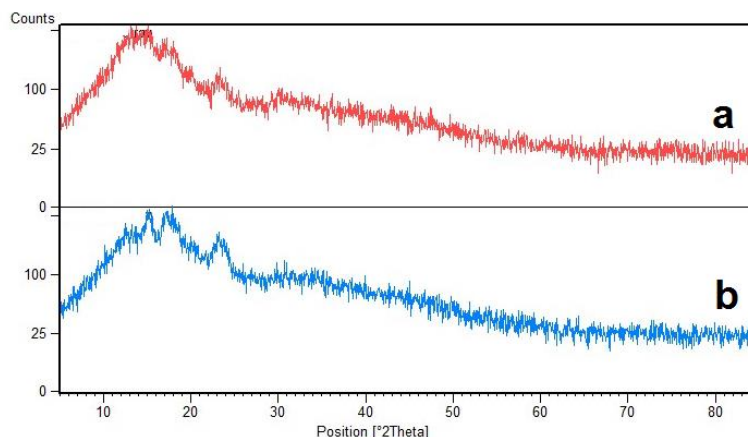


Fig. 4. X-ray diffraction pattern of potato starch powder (a) and synthesized starch phosphate (b)

The significance of each parameter was acquired by P-value. If the P-value is lower than 0.05 then this parameter is considered in the final model. CCD was employed to optimize the condition of the experiment and delineating associated graphs of the parameters.

The graphs retrieved from the RSM are exhibited in Fig. 5 for synthesized starch phosphate. Contour plots as an engagement of two parameters can express the relationship between different sorption variables and response, by maintaining the other parameters at the central level.

As shown in Fig. 5, the effects of the independent variables (temperature, adsorbent dosage, initial concentration of contaminant, pH, and time) at various levels were assessed on the response (removal efficiency of contaminant).

Fig. 5a shows the interaction effect of the initial concentration of contaminant (C_0) and pH on the removal efficiency of crystal violet for modified starch when the other factors are at a fixed values (temperature (T), contact time (t), and adsorbent dosage (C_s)) that designated that both of the independent factors significantly affect the removal efficiency. The contaminant removal efficiency of more than 90 percent takes place in the pH range of 2 to about 8 while increasing the initial concentration of crystal violet causes to decrease the removal efficiency. It was

recognized that in this pH range, on increasing the initial concentration to greater than 150 mgL^{-1} , the removal efficiency of crystal violet ions decreases. As when the range of crystal violet concentration was between 150–250 mg/L, the removal efficiency was less than 90% at pH lower than 4.0, but at higher pHs, removal percentage increased. Given that the pH at the point of zero charge (pH_{PZC}) for modified starch phosphate is 2.01 (Bahrami et al., 2019), the surface charge of adsorbent is negative in the studied range of pH. Besides, the crystal violet dye is cationic naturally (Rehman et al., 2017; Kulkarni et al., 2017), then it can easily interact with negatively charged surfaces of the adsorbent. Alike outcomes have been observed in the former studies (Saeed et al., 2010; Kulkarni et al., 2017).

Fig. 5b indicates the interaction effect of C_s and pH on the removal efficiency at fixed values of C_0 , t, and T. It is clear that the removal efficiency in each pH increases with enhancing the adsorbent amount, because the adsorption sites increases and leads to more removal of adsorbate (Bahrami et al., 2012). By 0.15 g of synthesized starch phosphate, more than 95% of crystal violet ions were eliminated in pH range of 5 to 7 while less than 80% removal was observed in alkaline and acidic pHs.

Figs. 5c and 5d show the contour and surface plot of interaction effect of C_s and

C_0 on removal efficiency at a fixed values of T , t , and pH , respectively. It is clear that at low initial concentrations of pollutant even with a low dosage of adsorbent, high values of efficiency can be achieved (more than 90%). The removal efficiency enhanced with ascending adsorbent dosage that can be attributed to the availability of more vacant adsorption sites (Bahrami et al., 2012; Bahrami et al., 2019). For a given C_s , the removal efficiency decreased with enhancing the C_0 due to the saturation of adsorption sites on the surface of the adsorbent and consequently no enough sites for interaction of adsorbate and adsorbent. Loqman et al. (2017) and Kulkarni et al.

(2017) indicated the similar findings about the removal of crystal violet by a local clay and water hyacinth, respectively.

Fig.5e illustrates the interaction effect of temperature and pH on removal efficiency at fixed values of C_0 , t , and C_s . As can be seen for all temperatures, the removal efficiency of more than 90 percent occurred at a pH range of 4 to 8 while the temperature had no significant effect on the removal efficiency.

The interaction effect of pH and contact time represented in Fig. 5f is also the case. As the high values of removal efficiencies were observed in the pH range of 4 to 8 and time had no significant effect.

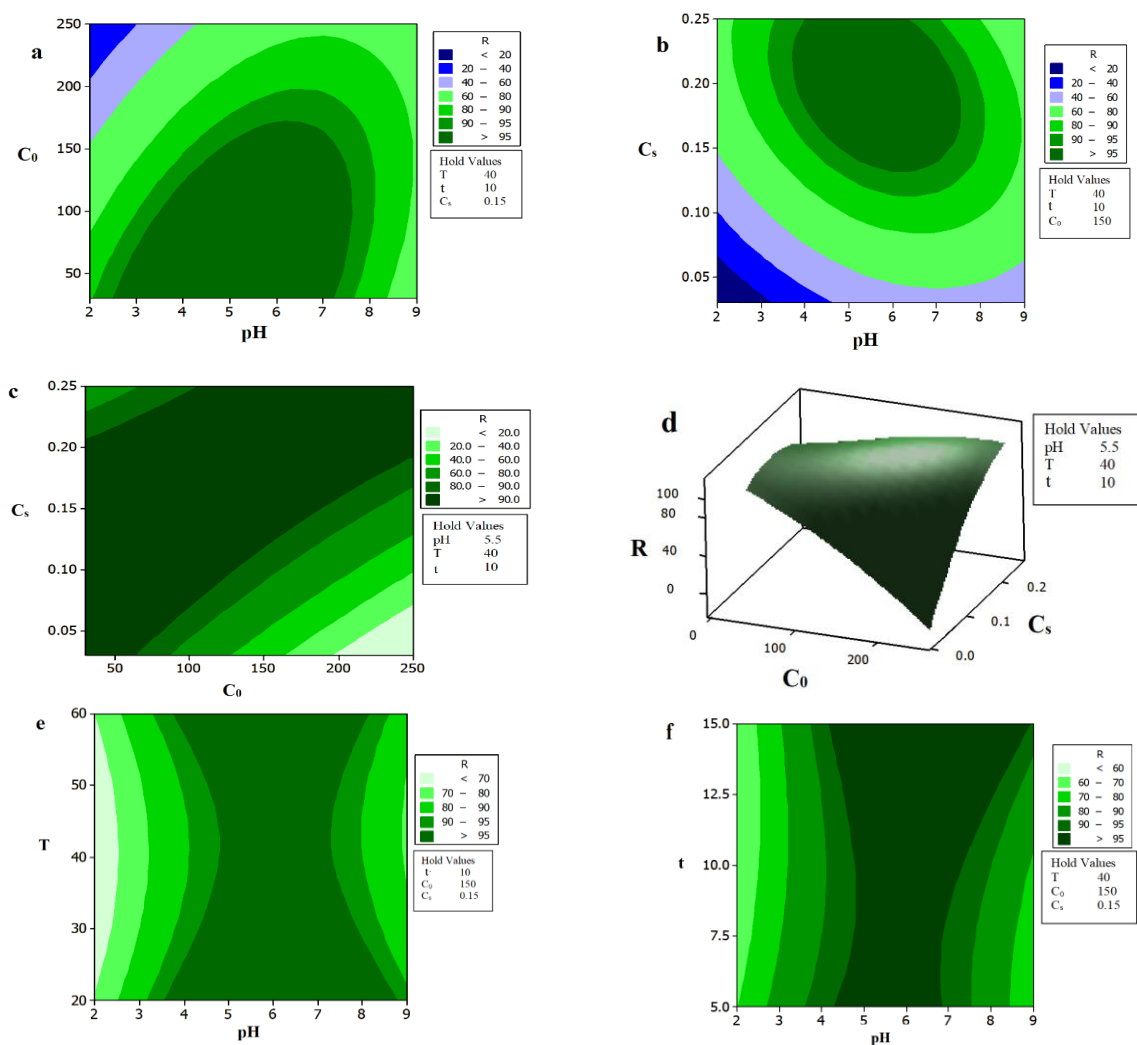


Fig. 5. Contour and surface plots for synthesized starch phosphate: a) interaction of C_0 * pH ; b) interaction of C_s * pH ; c) interaction of C_0 * C_s ; d) interaction of C_0 * C_s ; e) interaction of T * pH ; f) interaction of time* pH on R

To investigate the mechanism of crystal violet removal by synthesized starch phosphate, it is vital to comprehend the chemical structure of adsorbate and adsorbent. In this study, adsorption sites which cover the surface of S-S are OH groups and oxygen bridges (Fig. 6). There is a difference between the characteristics of adsorption sites in the sorption mechanism. The OH groups of adsorbent act as centers for adsorption through forming hydrogen bonds with the adsorbate. Generally, phosphorylation processes are evident due to the inclusion of phosphate groups inside the starch granules creating certain repulsive forces that enhance the inter- and

intramolecular spaces allowing more hydroxyl groups to be included.

Designating the optimal conditions of operating variables is the principal purpose of RSM. The optimum amount of each variable on the adsorption efficiency of crystal violet is designated by RSM to obtain the maximum dye removal efficiency (Fig. 7). The optimum level of five parameters for maximum crystal violet removal (99%) was achieved as initial crystal violet concentration= 213.54 mg/L, adsorbent dosage=0.25 g, contact time=14.99 min, temperature=15 °C, and initial pH of solution=9. The desirability score of the model was discovered to be 1, which confirms the accuracy of the RSM prediction.

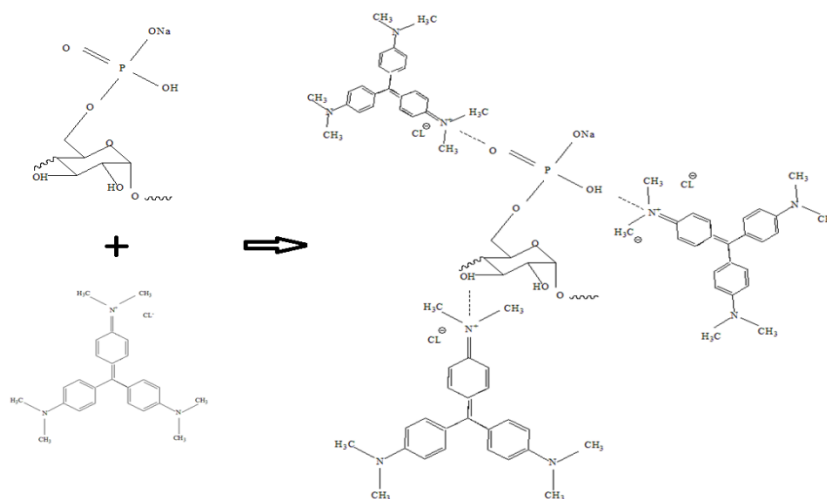


Fig. 6. Proposed adsorption mechanism of crystal violet dye on synthesized starch phosphate

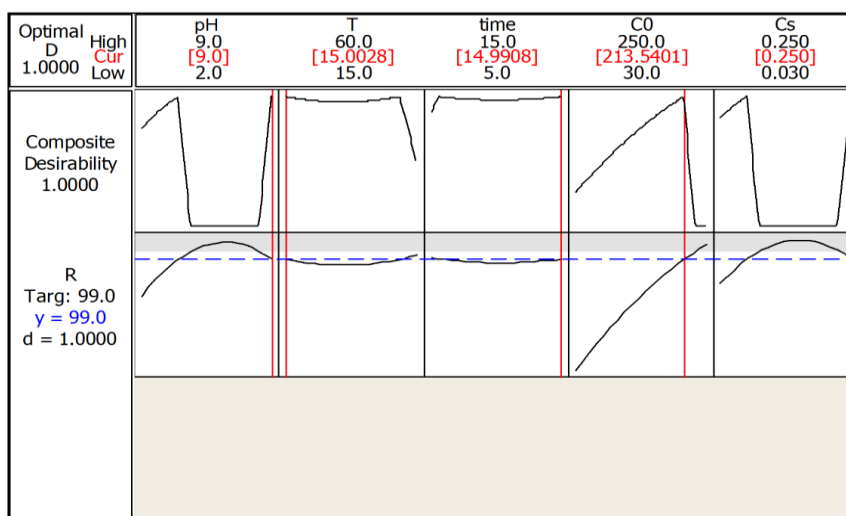


Fig. 7. Response optimization plot for the maximum adsorption of crystal violet by synthesized starch

CONCLUSION

In the present study, the performance of synthesized starch phosphate for removal of crystal violet dye from aqueous solution was investigated. Two parallel sets of experiments were carried out using RSM based on CCD to evaluate the effects of independent operational parameters, their interactions, and subsequently to establish the optimum conditions. The statistical analysis results proposed that a second-order polynomial regression model could properly interpret the experimental data.

The maximum adsorption efficiency of crystal violet ions was 99 % at the optimum adsorption conditions including initial crystal violet concentration 213.54 mg/L, adsorbent dosage 0.25 g, contact time 14.99 min, temperature 15 °C, and initial pH of solution 9.

Contour and surface plots indicated that the maximum removal efficiency of crystal violet ions could be obtained by raising pH and adsorbent dosage and decreasing the initial crystal violet concentration. Besides, surface plots showed that temperature and contact time are not effective variables in crystal violet removal from aqueous solutions using synthesized starch phosphate. These results are in agreement with Shojaei et al. (2019) that investigated the effects of parameters on the removal efficiency of crystal violet by nanozeolite-x via the Central Composite Design (CCD). Conclusively, the RSM model is proper to optimize the experiments for dye elimination by adsorption, where the modified starch phosphate would be an effective adsorbent for treating crystal violet solution.

GRANT SUPPORT DETAILS

The present research did not receive any financial support.

CONFLICT OF INTEREST

The authors declare that there is not any conflict of interests regarding the publication of this manuscript. In addition, the ethical issues, including plagiarism, informed

consent, misconduct, data fabrication and/ or falsification, double publication and/or submission, and redundancy has been completely observed by the authors.

LIFE SCIENCE REPORTING

No life science threat was practiced in this research.

REFERENCES

- Amiri, M.J., Bahrami, M. and Dehkhodaie, F. (2019). Optimization of Hg(II) adsorption on bio-apatite based materials using CCD-RSM design: characterization and mechanism studies. *J. Water Health*, 17 (4), 556-567.
- Amiri, M.J., Bahrami, M., Beigzadeh, B. and Gil, A. (2018). A response surface methodology for optimization of 2, 4-dichlorophenoxyacetic acid removal from synthetic and drainage water: a comparative study. *Environ. Sci. Pollut. Res.*, 25 (34), 34277-34293.
- Babaei, A.A., Bahrami, M., Farrokhan Firouzi, A., Ramazanpour Esfahani, A.H. and Alidokht, L. (2015). Adsorption of cadmium onto modified nanosized magnetite: kinetic modeling, isotherm studies, and process optimization. *J. Desalin. Water. Treatment*, 56, 3380–3392.
- Bahrami, M., Amiri, M.J. and Bagheri, F. (2019). Optimization of the lead removal from aqueous solution using two starch based adsorbents: design of experiments using response surface methodology (RSM). *J. Environ. Chem. Eng.*, 7, 102793.
- Bahrami, M., Boroomandnasab, S., Kashkuli, H.A., Farrokhan Firoozi, A. and Babaei, A.A. (2017). Removal of Cd (II) from aqueous solution using modified Fe₃O₄ nanoparticles. *Rep. Opin.*, 4 (5), 31-40.
- Bharathi, K.S. and Ramesh, S.T. (2013). Removal of dyes using agricultural waste as low-cost adsorbents: a review. *Appl. Water Sci.*, 3 (4), 773-790.
- Bhattacharjee, T., Gidde, M.R. and Bipinraj, N.K. (2013). Disinfection of drinking water in rural area using natural herbs. *International Journal of Engineering Research and Development*, 5 (10), 7-10.
- Coates, J. (2000). "Interpretation of Infrared Spectra, a Practical Approach," In R. A. Meyers, Ed., *Encyclopedia of Analytical Chemistry*, John Wiley & Sons Ltd, Chichester, 10815-10837.
- Crini, G. (2006). Non-conventional low-cost adsorbents for dye removal: a review. *Bioresour. Technol.*, 97 (9), 1061-85.
- Dehghani, M.H., Dehghan, A., Alidadi, H., Dolatabadi, M., Mehrabpour, M. and Converti, A.

- (2017). Removal of methylene blue dye from aqueous solutions by a new chitosan/zeolite composite from shrimp waste: Kinetic and equilibrium study. *Korean J. Chem. Eng.*, 34, 1699-1707.
- Duraipandian, J., Rengasamy, T. and Vadivelu, S. (2017). Experimental and modeling studies for the removal of crystal violet dye from aqueous solutions using eco-friendly *Gracilaria corticata* seaweed activated carbon/Zn/Alginate Polymeric composite beads. *Journal of polymers and the environment*, 25, 1062-1071.
- Feira, J.M.C.D., Klein, J.M. and Forte, M.M.D.C. (2018). Ultrasound-assisted synthesis of polyacrylamide-grafted sodium alginate and its application in dye removal. *Polímeros*, 28 (2), 139-146.
- Gil, A., Assis, F.C.C., Albeniz, S. and Korili, S.A. (2011). Removal of dyes from wastewaters by adsorption on pillared clays. *Chemical Engineering Journal*, 168 (3), 1032-1040.
- Gimbert, F., Crini, N., Renault, F., Badot, P. and Crini, G. (2008). Adsorption isotherm models for dye removal by cationized starch-based material in a single component system: Error analysis. *Journal of Hazardous Materials*, 157, 34-46.
- Kaur, S., Rani, S. and Mahajan, R.K. (2015). Adsorption of dye crystal violet onto surface-modified *Eichhornia crassipes*. *Desalin. Water Treat.*, 53 (7), 1957-1969.
- Kulkarni, M.R., Revanth, T., Acharya, A. and Bhat, P. (2017). Removal of crystal violet dye from aqueous solution using water hyacinth: Equilibrium, kinetics and thermodynamics study. *Resource-Efficient Technologies*, 3, 71-77.
- Loqman, A., El Bali, B., Lu'tzenkirchen, J., Weidler, P.G. and Kherbeche, A. (2017). Adsorptive removal of crystal violet dye by a local clay and process optimization by response surface methodology. *Appl. Water Sci.*, 7, 3649-3660.
- Mumbi, A.W., Fengting, L. and Karanja, A. (2018). Sustainable treatment of drinking water using natural coagulants in developing countries: A case of informal settlements in Kenya. *Water Utility Journal*, 18, 1-11
- Mundada, P. and Brighub, U. (2016). Remediation of textile effluent using siliceous materials: A review with a proposed alternative. *Int. J. Innov. Emerg. Res. Eng.*, 3 (1), 1-5.
- Murúa-Pagola, B., Beristain-Guevara, C.I. and Martínez-Bustos, F. (2009). Preparation of starch derivatives using reactive extrusion and evaluation of modified starches as shell materials for encapsulation of flavoring agents by spray drying. *J. Food Eng.*, 91, 380-386.
- Olad, A., Farshi Azhar, F., Shargh, M. and Jharfi, S. (2014). Application of Response Surface Methodology for modeling of reactive dye removal from solution using starch-montmorillonite/Polyaniline nanocomposite. *Polym. Eng. Sci.*, 54 (7), 1595-1607.
- Rabipour, M., Sekhvat Pour, Z. and Ghaemy, M. (2016). A novel PVA-based hydrogel nanocomposite for removal of crystal violet. 2nd international conference on new research in chemistry and chemical engineering. Tehran, Iran.
- Rehman, F., Sayed, M., Ali Khan, J. and Khan, H.M. (2017). Removal of crystal violet dye from aqueous solution by gamma irradiation. *J. Chil. Chem. Soc.*, 62 (1), 3359-3364.
- Saad, M., Tahir, H., Khan, J., Hameed, U. and Saud, A. (2017). Synthesis of Polyaniline nanoparticles and their application for the removal of crystal violet dye by Ultrasonicated adsorption process based on Response Surface Methodology. *Ultrasonics Sonochemistry*, 34, 600-608.
- Saeed, A., Sharif, M. and Iqbal, M. (2010). Application potential of grapefruit peel as dye sorbent: kinetics, equilibrium and mechanism of crystal violet adsorption. *J. Hazard. Mater.*, 179 (1), 564-572.
- Shahriari, T. and NabiBidhendi, G. (2012). Starch efficiency in water turbidity removal. *Asian Journal of Natural and Applied Sciences*, 1 (2), 134-137.
- Shojaei, S., Ahmadi, J., Davoodabadi Farahani, M., Mehdizadeh, B. and Pirkamali, M.R. (2019). Removal of crystal violet using nanozeolite-x from aqueous solution: Central composite design optimization study. *J. Water Environ. Nanotechnol.*, 4 (1), 40-47.
- Sofu, A. (2019). Investigation of dye removal with isolated biomasses from whey wastewater. *Int. J. Environ. Sci. Technol.*, 16 (1), 71-78.
- Song, X., He, G., Ruan, H. and Chen, Q. (2006). Preparation and properties of Octenyl Succinic Anhydride modified early *Indica* rice starch. *Starch/Stärke*, 58, 109-117.
- Sung, J.H., Park, D.P., Park, B.J., Choi, H.J. and Jhon, M.S. (2005). Phosphorylation of potato starch and its electrorheological suspension. *Biomacromolecules*, 6 (4), 2182-2188.
- Zehra, T., Priyantha, N. and Lim, L.B.L. (2016). Removal of crystal violet dye from aqueous solution using yeast-treated peat as adsorbent: thermodynamics, kinetics, and equilibrium studies *Environ. Earth Sci.*, 75, 357.

SUPPLEMENTARY MATERIALS

Table S1. Experimental values of variables designed by RSM model for original starch (S)

Run	pH	T (°C)	T (min)	C ₀ (mgL ⁻¹)	C _s (g)
1	5.5	40	67.5	40	0.3
2	5.5	40	67.5	40	0.3
3	4	30	45	55	0.2
4	7	50	45	25	0.2
5	7	50	90	25	0.2
6	7	50	45	55	0.2
7	4	50	45	25	0.4
8	4	30	90	55	0.4
9	7	50	90	55	0.2
10	4	30	45	25	0.2
11	7	30	45	25	0.4
12	7	50	45	55	0.4
13	7	30	90	55	0.2
14	4	30	45	25	0.4
15	7	30	90	25	0.2
16	7	30	90	55	0.4
17	4	50	45	55	0.2
18	4	30	90	55	0.2
19	4	50	90	55	0.4
20	4	50	90	55	0.2
21	7	30	90	25	0.4
22	5.5	40	67.5	40	0.3
23	4	30	90	25	0.2
24	7	50	90	55	0.4
25	4	50	90	25	0.2
26	4	30	90	25	0.4
27	5.5	40	67.5	40	0.3
28	4	50	90	25	0.4
29	7	50	45	25	0.4
30	7	30	45	55	0.2
31	5.5	40	67.5	40	0.3
32	5.5	40	67.5	40	0.3
33	4	50	45	55	0.4
34	5.5	40	67.5	40	0.3
35	5.5	40	67.5	40	0.3
36	4	30	45	55	0.4
37	4	50	45	25	0.2
38	7	50	90	25	0.4
39	7	30	45	55	0.4
40	7	30	45	25	0.2
41	5.5	40	15	40	0.3
42	9	40	67.5	40	0.3
43	5.5	40	67.5	40	0.3
44	5.5	40	67.5	40	0.3
45	5.5	40	67.5	40	0.3
46	2	40	67.5	40	0.3
47	5.5	40	67.5	80	0.3
48	5.5	40	120	40	0.3
49	5.5	40	67.5	40	0.5
50	5.5	20	67.5	40	0.3
51	5.5	40	67.5	5	0.3
52	5.5	40	67.5	40	0.3
53	5.5	60	67.5	40	0.3
54	5.5	40	67.5	40	0.06

Table S2. Experimental values of variables designed by RSM model for modified starch phosphate (S-S)

Run	pH	T (°C)	T (min)	C ₀ (mgL ⁻¹)	C _s (g)
1	7	50	12	200	0.2
2	7	30	12	200	0.2
3	4	50	12	100	0.1
4	7	50	12	200	0.1
5	5.5	40	10	150	0.15
6	5.5	40	10	150	0.15
7	4	50	8	200	0.1
8	4	30	8	200	0.2
9	4	50	8	100	0.2
10	7	30	12	200	0.1
11	4	50	12	200	0.2
12	7	50	8	100	0.1
13	4	30	12	200	0.2
14	4	30	8	100	0.2
15	4	30	12	200	0.1
16	7	30	8	100	0.2
17	7	50	8	200	0.1
18	7	50	8	200	0.2
19	4	30	12	100	0.2
20	4	50	8	200	0.2
21	5.5	40	10	150	0.15
22	7	30	8	200	0.1
23	4	30	8	200	0.1
24	7	30	12	100	0.1
25	4	30	12	100	0.1
26	7	30	8	200	0.2
27	7	50	12	100	0.2
28	5.5	40	10	150	0.15
29	4	30	8	100	0.1
30	7	30	8	100	0.1
31	5.5	40	10	150	0.15
32	4	50	12	100	0.2
33	4	50	12	200	0.1
34	7	30	12	100	0.2
35	7	50	8	100	0.2
36	7	50	12	100	0.1
37	5.5	40	10	150	0.15
38	5.5	40	10	150	0.15
39	5.5	40	10	150	0.15
40	4	50	8	100	0.1
41	5.5	40	10	150	0.03
42	5.5	40	10	150	0.15
43	5.5	40	10	150	0.15
44	9.0	40	10	150	0.15
45	5.5	40	10	150	0.15
46	5.5	60	10	150	0.15
47	5.5	20	10	150	0.15
48	5.5	40	15	150	0.15
49	2	40	10	150	0.15
50	5.5	40	10	150	0.15
51	5.5	40	10	30	0.15
52	5.5	40	10	250	0.15
53	5.5	40	5	150	0.15
54	5.5	40	10	150	0.25



Pollution is licensed under a "Creative Commons Attribution 4.0 International (CC-BY 4.0)"